Support Information

Phase control of solid-solution RuIn nanoparticles and their catalytic properties

Xin Zhou,[a] Megumi Mukoyoshi,*[a] Kohei Kusada,[a,b,c] Tomokazu Yamamoto,[d] Takaaki Toriyama,[d] Yasukazu Murakami,[d,e] and Hiroshi Kitagawa*[a]

[a.] *Division of Chemistry, Graduate School of Science, Kyoto University, Kitashirakawa-Oiwakecho, Sakyo-ku, Kyoto 606-8502, Japan.*

[b.] *The HAKUBI Center for Advanced Research, Kyoto University, Kitashirakawa-Oiwakecho, Sakyo-ku, Kyoto 606-8502, Japan.*

[c.] *JST-PRESTO, Honcho 4-1-8, Kawaguchi, Saitama 332-0012, Japan.*

[d.] *The Ultramicroscopy Research Center, Kyushu University, 744 Motooka, Nishi-ku, Fukuoka 819-0395, Japan.*

[e.] *Department of Applied Quantum Physics and Nuclear Engineering, Kyushu University, 744 Motooka, Nishi-ku, Fukuoka 819-0395, Japan.*

Table of Contents

Experimental Details 3

Figure S1. Rietveld refinement analysis of fcc RuIn NPs/C 7

Figure S2. Rietveld refinement analysis and TEM image of Ru NPs 8

Figure S3. Rietveld refinement analysis of hcp RuIn NPs/C 9

Figure S4. Rietveld refinement analysis of RuIn NPs/C (vacuum) 10

Figure S5. PXRD patterns of the RuIn NPs/C at different heating temperatures.....11

Figure S6. TEM images of fcc and hcp RuIn NPs/C 12

Figure S7. In 3d XPS spectra of fcc and hcp RuIn NPs/C.....13

Figure S8. Ru 3p XPS spectra of Ru NPs/C, fcc and hcp RuIn NPs/C 14

Figure S9. HER mass activity.....15

Figure S10. Chronoamperometry measurement of fcc RuIn NPs/C.....16

Figure S11. Chronoamperometry measurement of hcp RuIn NPs/C 17

Figure S12. XPS spectra of hcp and fcc RuIn NPs/C after the stability test 18

Figure S13. CV curves of ECSA measurement 19

Figure S14. TOF of Ru NPs/C, fcc and hcp RuIn NPs/C 20

Figure S15. VB-XPS spectra of commercial Pt NPs/C 21

References.....22

Experimental Details

Chemicals

Ruthenium chloride ($RuCl_3 \cdot nH_2O$) and indium chloride tetrahydrate ($InCl_3 \cdot 4H_2O$) were purchased from Wako Pure Chemical Industries, Ltd. (Japan). Ruthenium (III) acetylacetonate ($Ru(C_5H_7O_2)_3$, $Ru(acac)_3$), glucose ($C_6H_{12}O_6$) and benzyl ether ($C_{14}H_{14}O$) were purchased from Sigma-Aldrich Chemical Co. (USA). Oleylamine ($C_{18}H_{37}N$, OAm) was purchased from Thermo Fisher Scientific Co. Ltd. (USA). Commercial platinum 20 wt% on carbon (commercial Pt NPs/C) was purchased from Johnson Matthey Co., Ltd. (UK). All reagents were used as received without further purification.

Characterization

Transmission electron microscopy (TEM) images were obtained using a Hitachi HT7700 instrument at 100 kV.

High-angle annular dark-field scanning transmission electron microscopy (HAADF-STEM) images and energy-dispersive X-ray (EDX) spectra were acquired using a JEOL JEM-ARM200CF STEM instrument (120 kV), equipped with an aberration corrector, at Kyushu University (Japan).

Powder X-ray diffraction (XRD) was conducted with a Rigaku MiniFlex 600 diffractometer equipped with a Cu Kα radiation source (λ = 1.5405(9) Å). Rietveld refinements were carried out using the TOPAS3 software developed by Bruker AXS GmbH (Karlsruhe, Germany).

X-ray fluorescence (XRF) was measured with a Rigaku ZSX Primus IV instrument.

X-ray photoelectron spectroscopy (XPS) and valence-band X-ray photoelectron spectroscopy (VB-XPS) results were recorded using a Shimadzu ESCA-3400 X-ray photoelectron spectrometer, with a Mg Kα anode. The binding energy (BE) was corrected with the reference to the C (1s) peak at 284.6 eV. The VB-XPS spectra of carbon powder was also measured to remove the background. All the VB spectra were normalized in the spectral area at a BE from 12.0 to −2.0 eV.

Synthesis of fcc RuIn/C NPs

In a typical synthesis, a mixture of 30.0 mL of OAm containing 3.0 mmol of

glucose was first evacuated for 1 h at 100°C and then heated to 320°C. Next, 0.16 mmol $Ru(acac)_3$ and 0.04 mmol $InCl_3 \cdot 4H_2O$ were dissolved in a mixture of 10.0 mL OAm and 5.0 mL benzyl ether, affording a metal precursor mixture. The metal precursor mixture was then added dropwise at a rate of 0.5 mL min^{-1} into the preheated OAm solution. Upon completion of the addition, the reaction was maintained at 320°C for a further 1 h. The synthesis process was conducted under a continuous flow of Ar. Here, the OAm and glucose act as reducing agents and surfactants. The obtained powder was washed with hexane and ethanol, and the black powder was collected after centrifugation at 7800 rpm.

Next, the obtained black powder was loaded onto commercial carbon black. Details of the loading process are explained in the Electrochemical measurements section of the Support Information. The carbon-loaded black powder was cleaned by cyclic voltammetry (CV) at a voltage of 0.05–0.4 V (vs RHE: reversible hydrogen electrode) with a rate of 500 mV/s for several hundreds of cycles to remove the surface oxides, until a stable CV curve was obtained. Finally, the black powder after the CV cleaning was collected.

Synthesis of hcp RuIn NPs/C

To obtain the hcp RuIn NPs/C, the as-synthesized black powder was collected and sealed in a 100-kPa H_2 atmosphere and heated at 723 K for 1.5 h. For comparison, the as-synthesized black powder was also heated at 723 K for 1.5 h under vacuum conditions. The black powders after the heat treatment were collected.

Synthesis of hcp Ru NPs

In a typical synthesis, 0.5 mmol of $RuCl_3 \cdot nH_2O$ was first dissolved into 50 mL of the OAm solution with 3.0 mmol of glucose. Then, the mixture was heated to 320°C and maintained under magnetic stirring for 3 h. Finally, the black powder was collected by washing with hexane and ethanol and centrifugation at 7800 rpm.

Electrochemical measurements

The electrochemical process of the HER was carried out at room temperature using an electrochemical analyser (CHI760E, CH Instruments, USA) and

repeated three times. A three-electrode system was adopted for the electrochemical measurements, with a rotating disk electrode (diameter 5 mm), Ag/AgCl (saturated KCl), and a graphite rod as the working electrode, reference electrode and counter electrode, respectively.

To prepare the carbon-loaded catalyst sample, the obtained black powder was loaded (metal percentage of ~20 wt%) onto commercial carbon black (Vulcan XC-72R). The carbon black and the obtained NPs were first dispersed in hexane and sonicated for 3 h. After a further 12 h of stirring, the product was washed three times with ethanol, collected by centrifugation and then dried overnight under vacuum conditions. Next, to remove excess surfactant, the obtained black powder was further treated for 2 h at 60°C in a 0.5 M acetic acid solution under an Ar atmosphere.[1] The acquired carbon-loaded powder was washed three times with ethanol and collected by centrifugation at 7800 rpm.

Next, 5.0 mg of the above carbon-loaded sample was dispersed into a mixture of isopropanol (1.6 mL), water (0.3 mL) and 5 wt% Nafion solution (0.1 mL) and was sonicated for 2 h in an ice water bath to prepare the catalyst ink for electrochemical measurements. Subsequently, 10.0 μL of the catalyst ink was dropped onto a glassy carbon electrode (diameter 5 mm, polished with diamond and Al_2O_3 solutions sequentially prior to use) and dried overnight. The mass loading density of RuIn NPs/C on a glassy carbon electrode is 0.1276 mg/cm^{-2} (corresponds to 0.0255 mg/cm^{-2} for RuIn NPs).

All measurements were carried out in a 0.5 M H_2SO_4 electrolyte. The 0.5 M H_2SO_4 electrolyte was bubbled with Ar for 40 min prior to the electrochemical process. First, the working electrode was cleaned by a CV scan at 0.05–0.40 V (vs RHE) for several hundred cycles at a rate of 500 mV/s until a stable CV curve was obtained. The linear scanning voltammetry curves were recorded at a scan rate of 5 mV/s and potentials ranging from 0.05 to –0.20 V (vs RHE). The durability of the catalyst was tested by chronoamperometry measurements for 10 h. 85% of the ohmic drop (iR) compensation was corrected for the data.

The turnover frequency (TOF) of the catalyst was derived from the electrochemically active surface area (ECSA) measured via the copper underpotential deposition (Cu UPD) method.[2–4]

The ECSA, active sites (n) and TOF were calculated from equations (1), (2) and (3), respectively:

$$ECSA = \frac{Q_{cu}}{0.42\ mC \cdot cm^{-2}} = \frac{\int_{E_1}^{E_2} I(E)d(E)}{v \cdot 0.42\ mC \cdot cm^{-2}} \quad (1)$$

$$n = \frac{Q_{cu}}{2F} \quad (2)$$

$$TOF = \frac{I}{2Fn} \quad (3)$$

where Q_{Cu} is the voltammetry charge of Cu UPD after deducting the blank CV profile in pure Ar-saturated 0.5 M H_2SO_4. I is the current measured by linear scanning voltammetry. The value of 0.42 mC cm^{-2} is the conversion factor for the Cu deposition process. F is the Faraday constant (96,485 C mol^{-1}). E_1 and E_2 are the lower and upper limits of voltage for Cu UPD, respectively. And v is the scan rate of CV. A factor of 2 is included in equations (2) and (3) because two electrons are required to form a hydrogen molecule.

Details of the Cu UPD experiment are as follows. First, the electrodes were subjected to several hundreds of CV scans in an Ar-saturated 0.5 M H_2SO_4 solution at a high rate of 500 mV/s in the range of 0.05–1.00 V (vs RHE) to remove surface oxides. Then several CV fine scans in the range of 0.05–1.00 V were recorded at a rate of 10 mV/s in an Ar-saturated 0.5 M H_2SO_4 solution. The electrodes were then transferred to an Ar-saturated electrolyte of 0.5 M H_2SO_4 containing 5 mM $CuSO_4$ and polarized for 100 s at a selected deposition potential to form a Cu monolayer. Finally, the Cu monolayer was stripped by CV scanning at a rate of 10 mV/s from the fixed potential to the upper potential.

Valence-band X-ray photoelectron spectroscopy

The d-band centre of the catalyst could be calculated based on the following equation (4):[5–7]

$$\overline{E}_{d-band} = -\frac{\int E \times DOS(E)dE}{\int DOS(E)dE} \quad (4)$$

where E is the binding energy and DOS(E) is the density of states (DOS) of the occupied d-states. In this work, we denote DOS(E) by the observed VB-XPS spectral intensity I(E), and the gravity centre of the VB-XPS spectrum is defined as the observed d-band centre. Therefore, the observed d-band centre can be derived from the following equation (5):

$$\overline{E}_{d-band}^{obs} = -\frac{\int E \times I(E)dE}{\int I(E)dE} \quad (5)$$

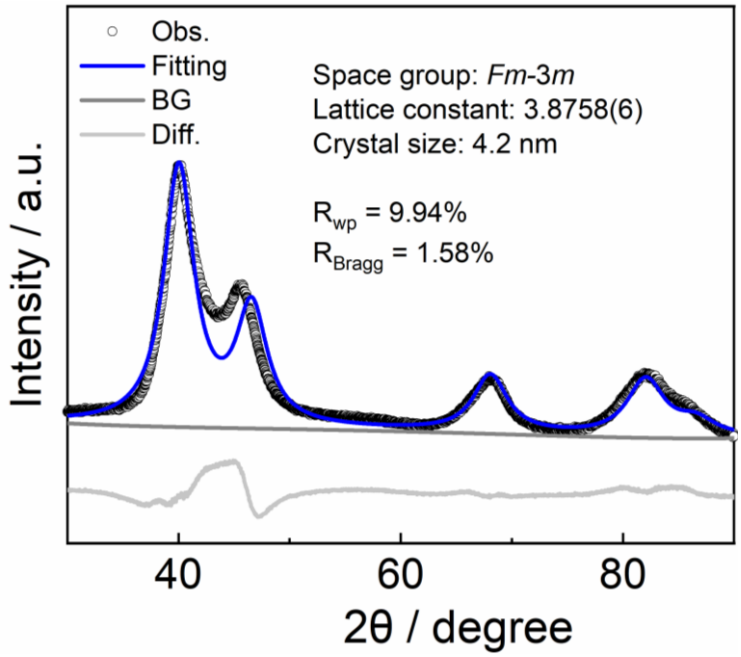

Fig. S1 Rietveld refinement analysis of fcc RuIn NPs/C.

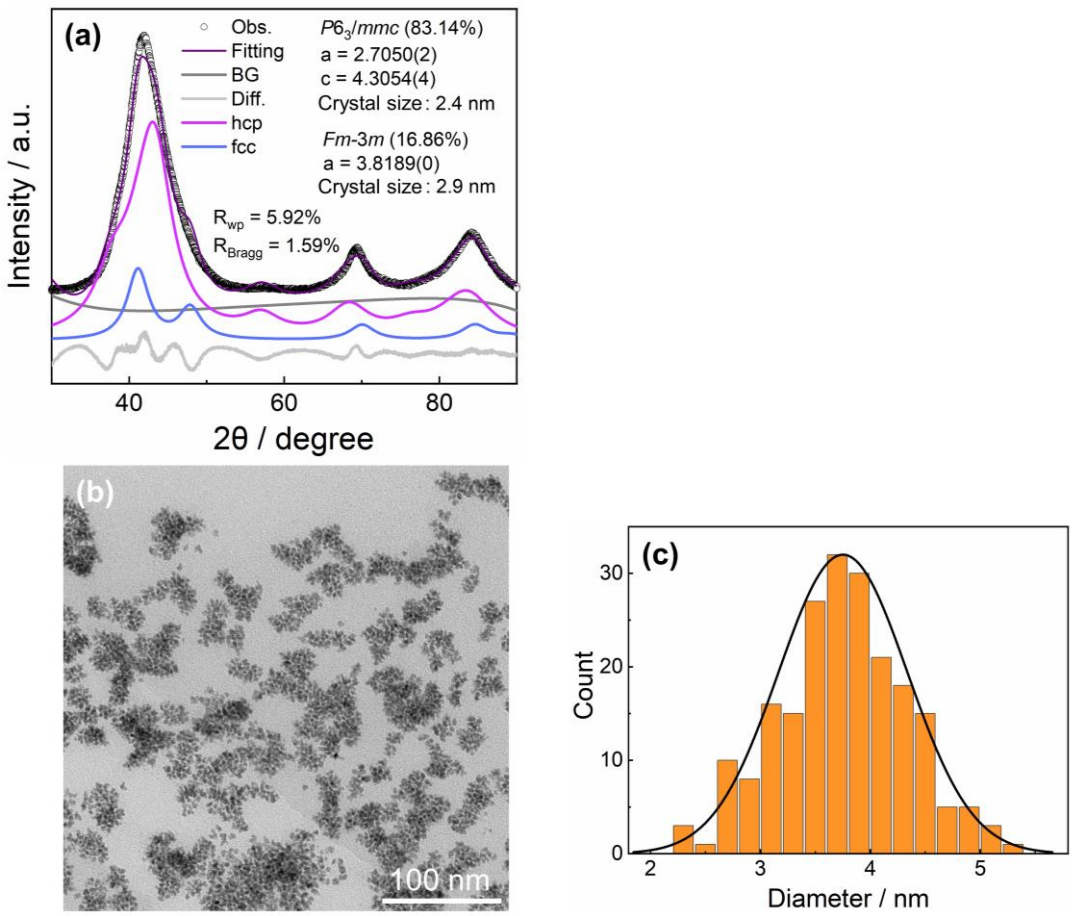

Fig. S2 (a) Rietveld refinement analysis of hcp Ru NPs. (b) TEM image of the hcp Ru NPs. (c) Histogram of the particle size distribution of hcp Ru NPs.

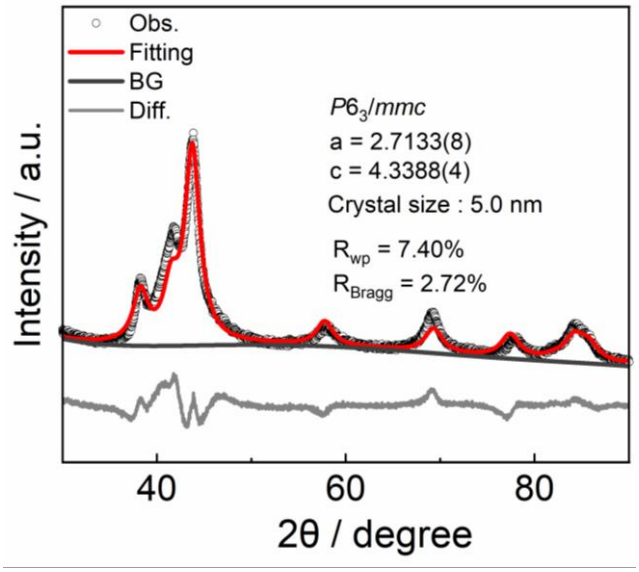

Fig. S3 Rietveld refinement analysis of hcp RuIn NPs/C.

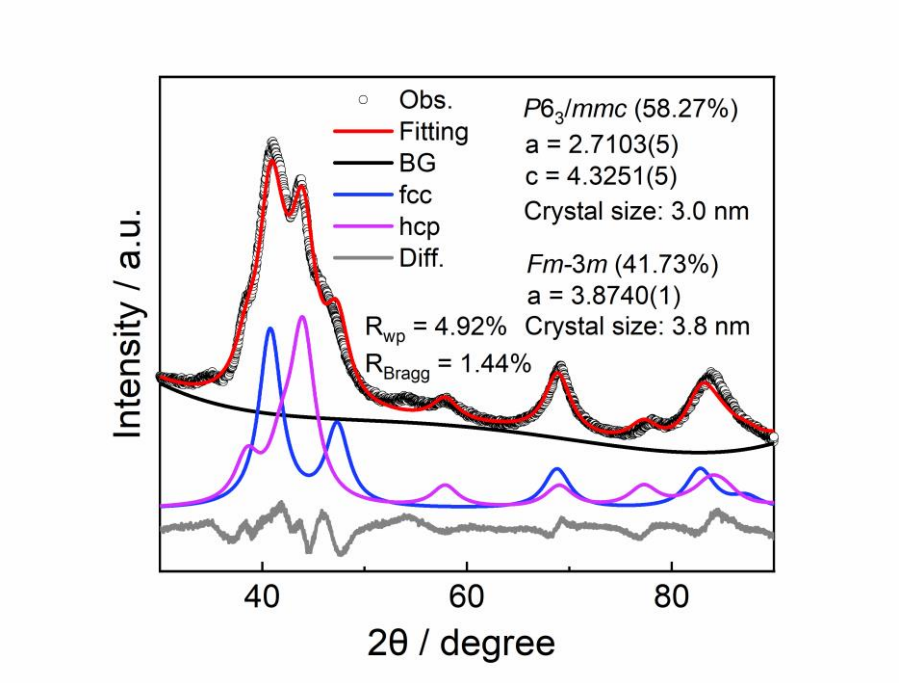

Fig. S4 Rietveld refinement analysis of RuIn NPs/C heated under a vacuum condition.

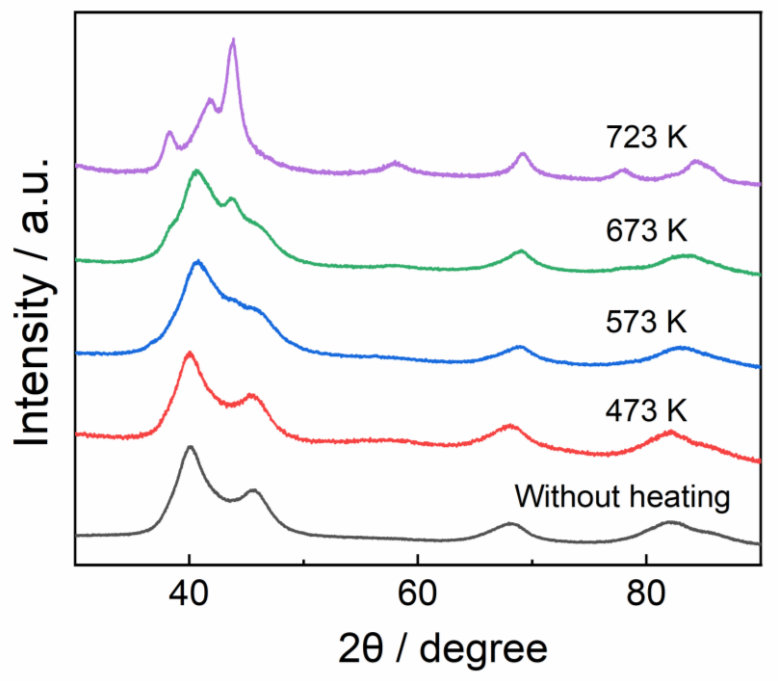

Fig. S5 PXRD patterns of the RuIn NPs/C at different heating temperatures for 1.5 h.

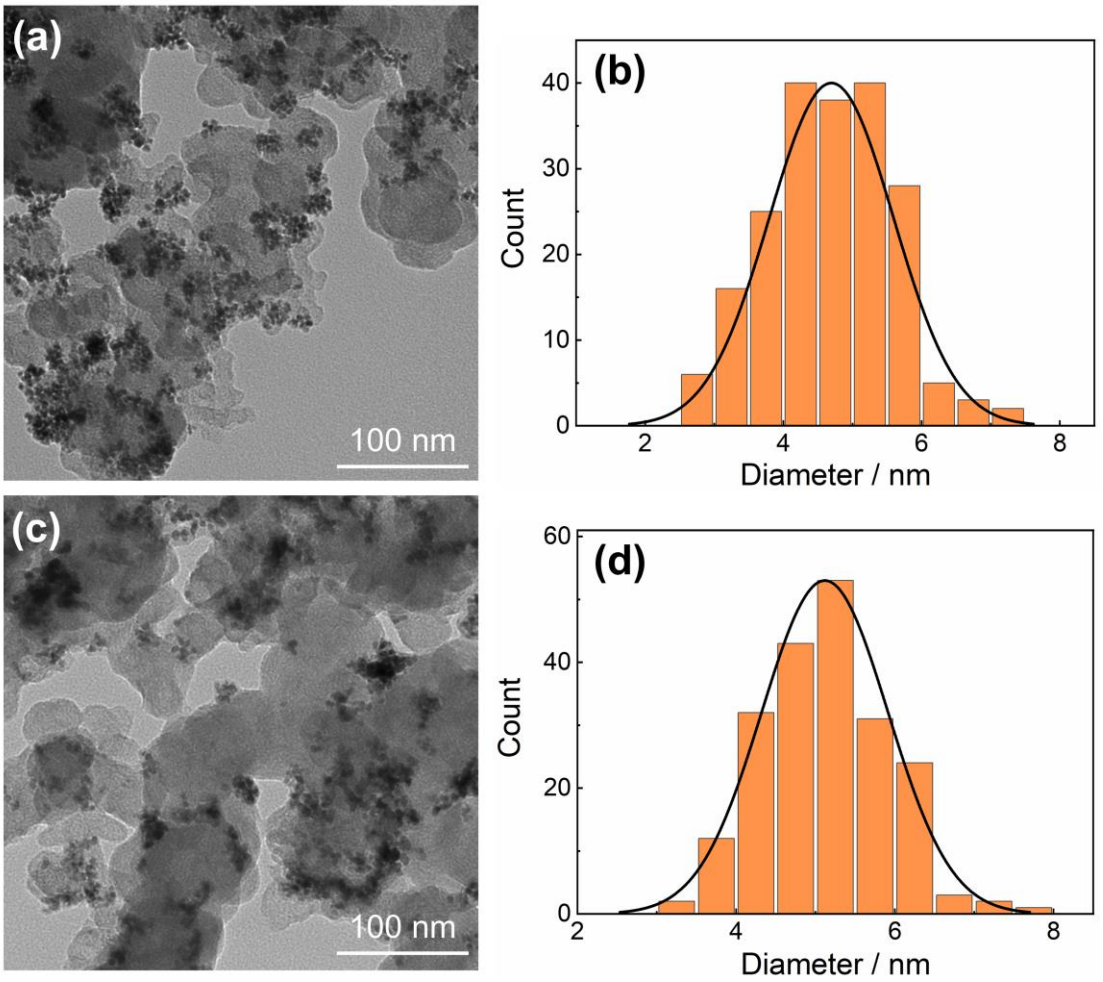

Fig. S6 (a) TEM image of fcc RuIn NPs/C. (b) Histogram of the particle size distribution of fcc RuIn NPs/C. (c) TEM image of hcp RuIn NPs/C. (d) Histogram of the particle size distribution of hcp RuIn NPs/C.

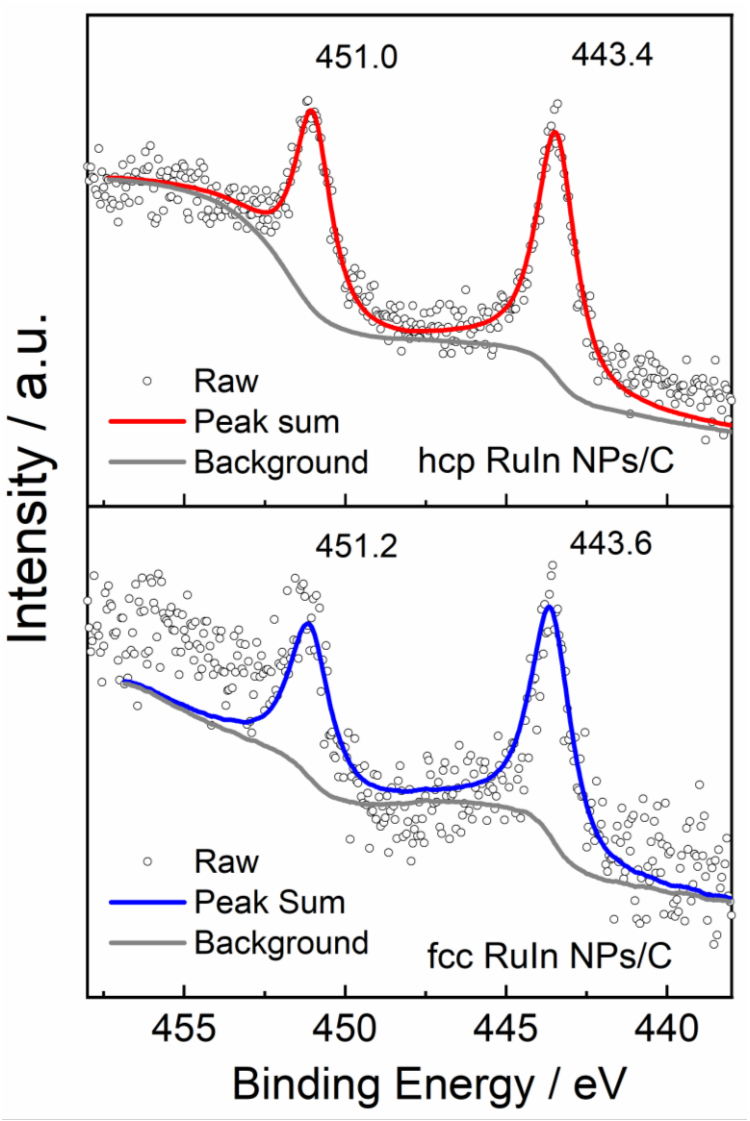

Fig. S7 In 3d XPS spectra of fcc RuIn NPs/C (blue) and hcp RuIn NPs/C (red).

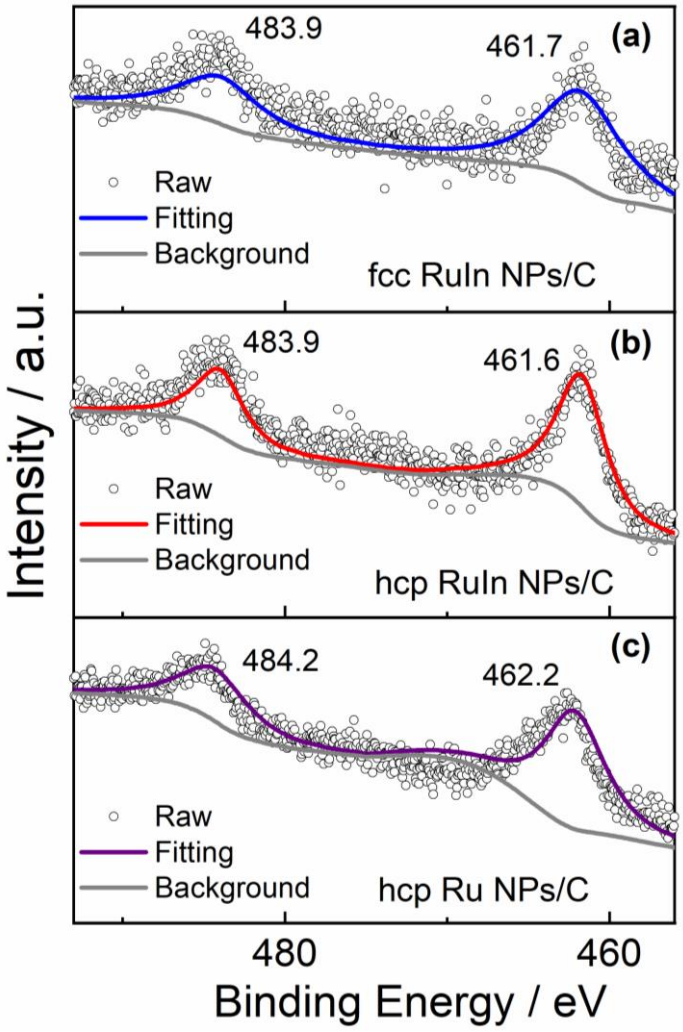

Fig. S8 Ru 3p XPS spectra of (a) fcc RuIn NPs/C (blue), (b) hcp RuIn NPs/C (red) and (c) hcp Ru NPs/C (brown).

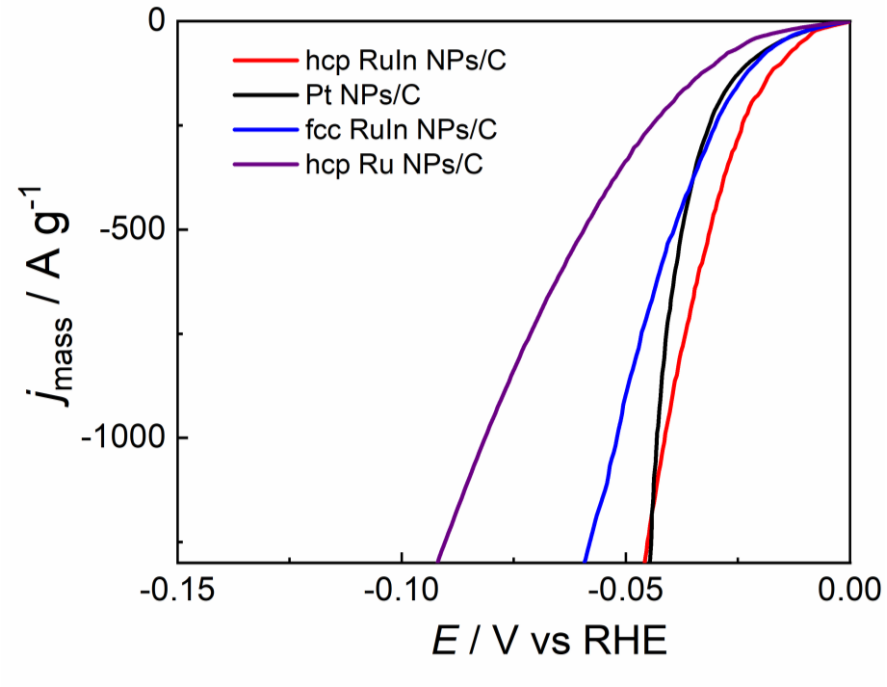

Fig. S9 HER mass activity of hcp RuIn NPs/C, fcc RuIn NPs/C, commercial Pt NPs/C and hcp Ru NPs/C.

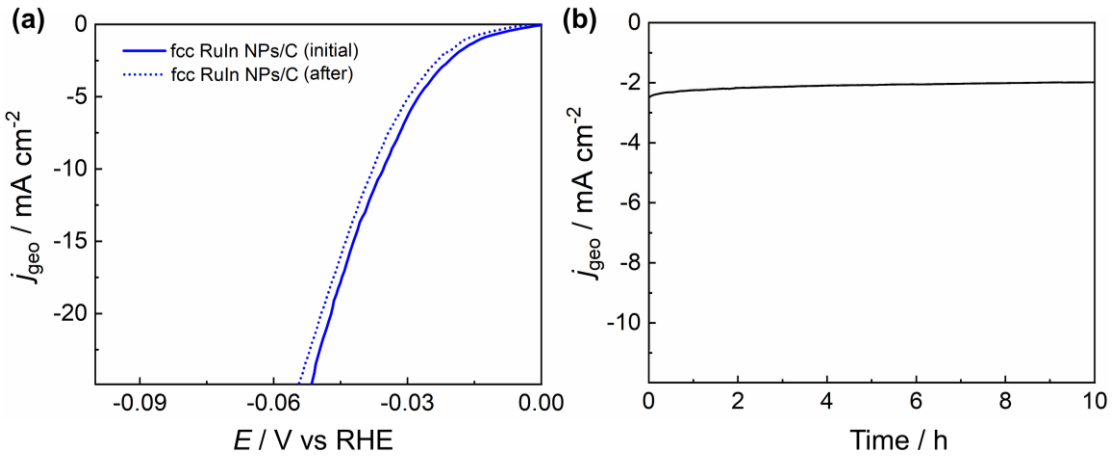

Fig. S10 (a) Polarization curves of fcc RuIn NPs/C before and after the durability test. (b) Chronoamperometry measurement of fcc RuIn NPs/C at a potential of –10 mV (vs RHE).

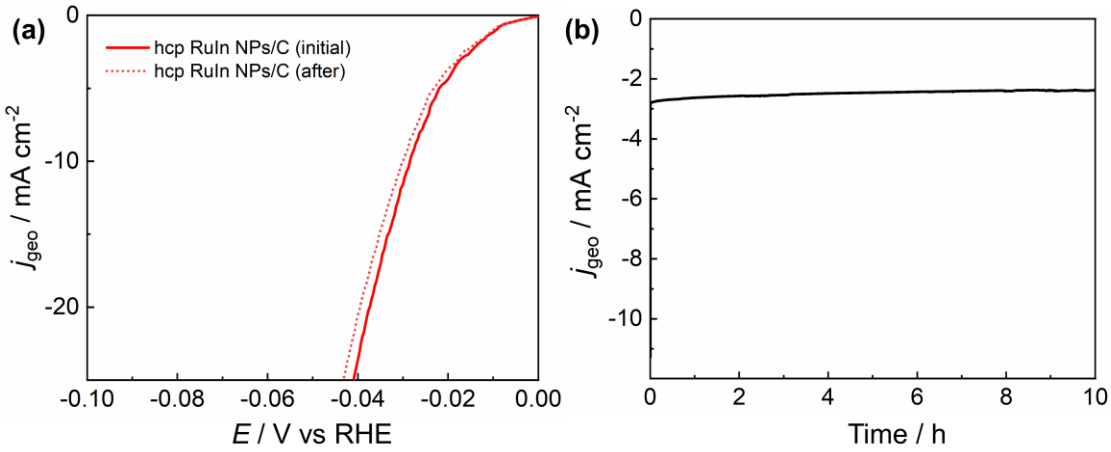

Fig. S11 (a) Polarization curves of hcp RuIn NPs/C before and after the durability test. (b) Chronoamperometry measurement of hcp RuIn NPs/C at a potential of –10 mV (vs RHE).

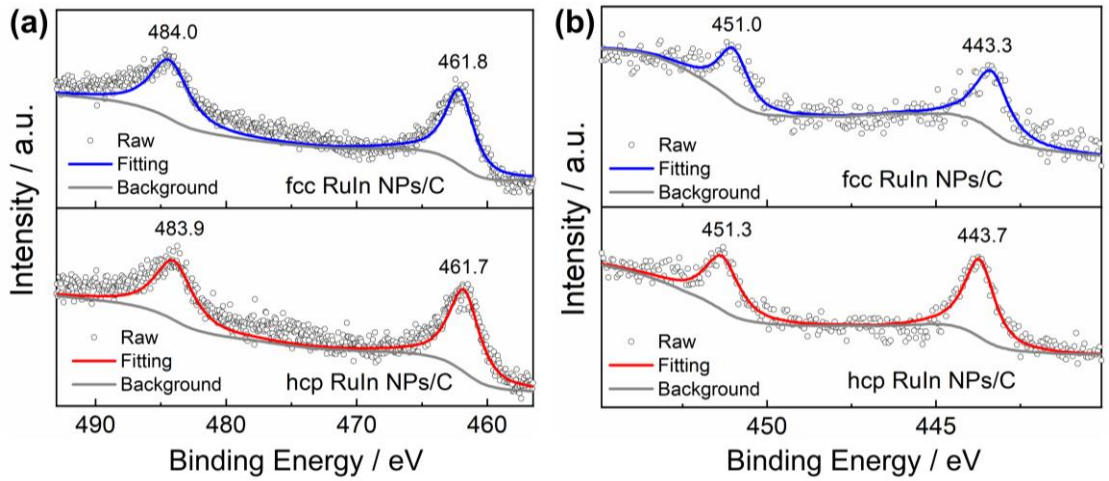

Fig. S12 XPS spectra of (a) Ru 3p and (b) In 3d of hcp and fcc RuIn NPs/C after the stability test.

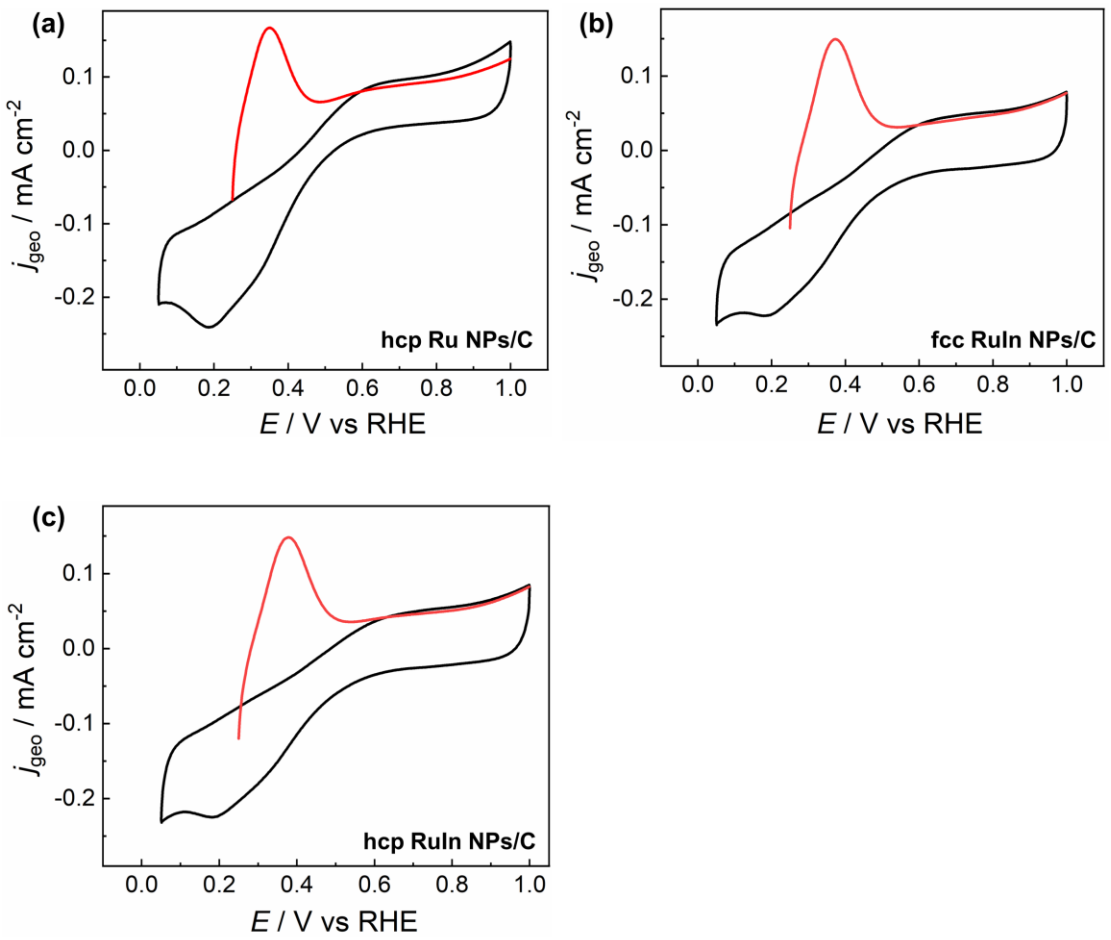

Fig. S13 ECSA measurements of CV curves for (a) hcp Ru NPs/C, (b) fcc RuIn NPs/C and (c) hcp RuIn NPs/C. The black CV curves were obtained in an Ar-saturated 0.5 M H_2SO_4 solution, and the red CV curves were obtained in an Ar-saturated 0.5 M H_2SO_4 solution containing 5 mM $CuSO_4$.

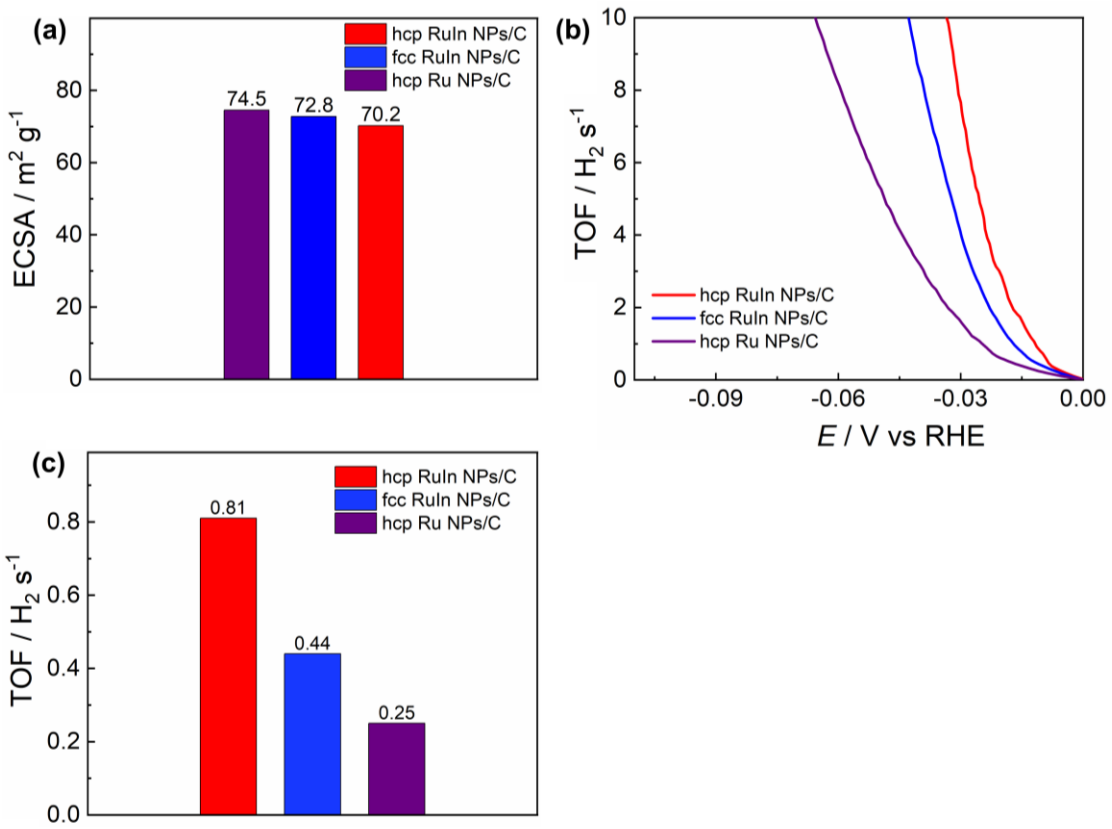

Fig. S14 (a) ECSA of hcp Ru NPs/C, fcc RuIn NPs/C and hcp RuIn NPs/C. (b) TOF of hcp Ru NPs/C, fcc RuIn NPs/C and hcp RuIn NPs/C. (c) TOF values of hcp Ru NPs/C, fcc RuIn NPs/C and hcp RuIn NPs/C at an overpotential of 10 mV.

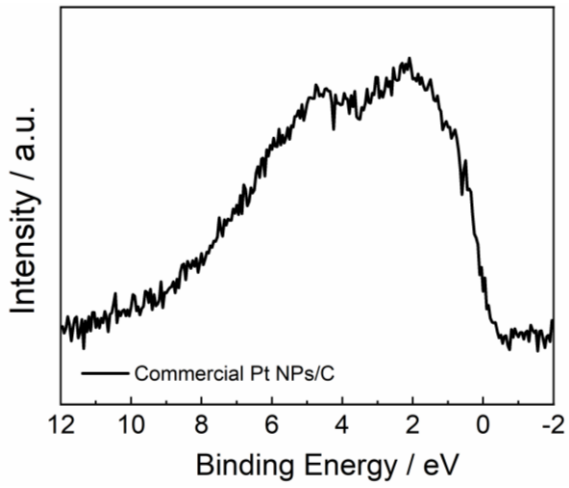

Fig. S15. VB-XPS spectra of commercial Pt NPs/C.

References:

1. M. Luo, Z. Zhao, Y. Zhang, Y. Sun, Y. Xing, F. Lv, Y. Yang, X. Zhang, S. Hwang, Y. Qin, J. Y. Ma, F. Lin, D. Sun, G. Lu and S. Guo, *Nature*, 2019, **574**(7776), 81–85.
2. Y. Zheng, Y. Jiao, Y. Zhu, L. H. Li, Y. Han, Y. Chen, M. Jaroniec and S. Z. Qiao, *J. Am. Chem. Soc.*, 2016, **138**(49), 16174–16181.
3. H. Minamihara, K. Kusada, D. Wu, T. Yamamoto, T. Toriyama, S. Matsumura, L. S. R. Kumara, K. Ohara, O. Sakata, S. Kawaguchi, Y. Kubota and H. Kitagawa, *J. Am. Chem. Soc.*, 2022, **144**(26), 11525–11529.
4. Z. Zhuang, Y. Wang, C. Q. Xu, S. Liu, C. Chen, Q. Peng, Z. Zhuang, H. Xiao, Y. Pan, S. Lu, R. Yu, W. C. Cheong, X. Cao, K. Wu, K. Sun, Y. Wang, D. Wang, J. Li and Y. Li, *Nat. Commun.,* 2019, **10**, 4875.
5. D. Wu, K. Kusada, S. M. Aspera, H. Nakanishi, Y. Chen, O. Seo, C. Song, J. Kim, S. Hiroi, O. Sakata, T. Yamamoto, S. Matsumura, Y. Nanba, M. Koyama, N. Ogiwara, S. Kawaguchi, Y. Kubota and H. Kitagawa, *ACS Mater. Au*, 2021, **2**(2), 110–116.
6. C. Song, A. Tayal, O. Seo, J. Kim, Y. Chen, S. Hiroi, L. S. R. Kumara, K. Kusada, H. Kobayashi, H. Kitagawa and O. Sakata, *Nanoscale Adv.*, 2019, **1**(2), 546–553.
7. D. Wu, K. Kusada, T. Yamamoto, T. Toriyama, S. Matsumura, I. Gueye, O. Seo, J. Kim, S. Hiroi, O. Sakata, S. Kawaguchi, Y. Kubota and H. Kitagawa, *Chem. Sci.*, 2020, **11**(47), 12731–12736.